Instabilities of vortices in a binary mixture of trapped Bose-Einstein condensates: Role of collective excitations with positive and negative energies

Dmitry V. Skryabin*
Department of Physics and Applied Physics, University of Strathclyde, Glasgow G4 0NG, United Kingdom
(Received 19 January 2000; revised manuscript received 16 June 2000; published 7 December 2000)

Correspondence between frequency and energy spectra and biorthogonality conditions for the excitations of Bose-Einstein condensates described by the Gross-Pitaevskii model have been derived self-consistently using general properties arising from the Hamiltonian structure of the model. It has been demonstrated that frequency resonances of the excitations with positive and negative energies can lead to their mutual annihilation and appearance of the collective modes with complex frequencies and zero energies. Conditions for the avoided crossing of energy levels have also been discussed. General theory has been verified both numerically and analytically in the weak interaction limit considering an example of vortices in a binary mixture of condensates. Growth of excitations with complex frequencies leads to spiraling of the unit and double vortices out of the condensate center to its periphery and to splitting of the double- and higher order vortices to the unit-order vortices.

DOI: 10.1103/PhysRevA.63.013602 PACS number(s): 03.75.Fi, 67.40.Vs

I. INTRODUCTION

Recent observations of the quantized vortices in a dilute ultracold gas of ^{87}Rb atoms [1,2] are spectacular evidences of the superfluid properties of atomic gases below transition temperature for the formation of a Bose-Einstein condensate (BEC). The first experimental results were obtained using a method suggested by Williams and Holland [3], in a binary mixture of the hyperfine states of ^{87}Rb [1], and more recent experiments [2] have demonstrated vortices and vortex lattices in an optically stirred single-component condensate.

The Gross-Pitaevskii (GP) equation [4] is a widely used approximation to describe the dynamics of the quantized vortices in the superfluid component of Bose gases at temperatures below critical. The GP equation falls into a general class of Hamiltonian nonlinear systems. The theory of stability of stationary solutions (equilibria) of such systems is well established at the moment, see, e.g., [5]. However, a certain gap between formal mathematical knowledge and applications to physical examples still exists and BEC field is not an exception. One of the controversial examples in the BEC context is the complex or imaginary eigenfrequencies in the spectrum of elementary excitations. The existence of these frequencies was first pointed out by Bogoliubov in his original work [6]; for more recent references see, e.g., [7–11,31,12]. An unjustified negligence by the non-self-adjointness of the Bogoliubov equations often led to the association between frequencies and energies in a way that was standard for quantum mechanics based on self-adjoint operators, thus admitting the possibility of complex energies in a conservative system.

However, a rigorously proved theorem allowing a clear physical interpretation of the complex frequencies is known from the general theory of Hamiltonian systems [5]. It states that excitations with complex frequencies can appear only as a result of the resonance between two excitations with positive and negative energies [13]. The roots of this theorem go back to the 19th century [14] and it has been used for the interpretation of instabilities with complex eigenvalues in plasma physics [15] and fluid dynamics [16]. Motivated by recent experiments on the observation of vortices in a binary mixture of condensates [1], we will demonstrate that these vortices can have complex frequencies in their spectrum, thereby giving good practical grounds for a self-consistent theoretical interpretation of this phenomenon in the BEC context.

Properties of vortices in the single-component magnetically trapped ultracold gases have been subject to intensive theoretical investigations; see, e.g., [9,17–32], which significantly extended classical works [4,33] dealing with the spatially unbounded case. The properties of unit vortices in the two-component condensates have also been studied, parallel to and independently from this work, by Garcia-Ripoll and Pérez-Garcia [10,11]. The richness of the dynamics of the two-condensate system and different approaches to the problem have led to only a few overlaps, which are outlined where appropriate.

In the next section we introduce coupled GP equations and briefly describe their general properties. Then, in Sec. III, we derive Bogoliubov equations for excitations, clearly specifying differences between frequency and energy spectra of the excitations. We also explain the scenario of the appearance of excitations with complex frequencies and show that they have zero energies. In Sec. IV we verify the validity of general results presented in Sec. III using perturbation theory in the limit of weak interaction and direct numerical study of Bogoliubov equations. In Secs. IV and V we describe how long-term dynamics of unit- and higher-order vortices can be interpreted using linear Bogoliubov theory. A stability criterion for unit vortices, which is formally more rigorous, compared to the one given in [11], is also derived in Sec. IV.

II. GROSS-PITAEVSKII EQUATIONS

Studies of superfluid mixtures using coupled GP equations have a long history and have attracted significant recent

*URL: www://http.cnqo.strath.ac.uk/~dmitry

activities; see, e.g., [1,7,8,10,11,34–38], and references therein. Following these works we assume that the wave functions $\psi_{1,2}$ of a two-species condensate inside an axial harmonic trap obey

$$i\hbar\partial_t\psi_1 = -\frac{\hbar^2}{2m}\vec{\nabla}^2\psi_1 + \frac{1}{2}m\Omega^2(r^2+\sigma^2 z^2) + (u_{11}|\psi_1|^2 + u_{12}|\psi_2|^2)\psi_1, \quad (1)$$

$$i\hbar\partial_t\psi_2 = -\frac{\hbar^2}{2m}\vec{\nabla}^2\psi_2 + \frac{1}{2}m\Omega^2(r^2+\sigma^2 z^2) + (u_{22}|\psi_2|^2 + u_{21}|\psi_1|^2)\psi_2,$$

where for simplicity we have neglected the possible differences of atomic masses $m_{1,2}=m$ and trap frequencies $\Omega_{1,2}=\Omega$, $\sigma_{1,2}=\sigma$, $\vec{\nabla}=\vec{i}_x\partial_x+\vec{i}_y\partial_y+\vec{i}_z\partial_z$, $r^2=x^2+y^2$. Coefficients $u_{ij}=4\pi\hbar^2 a_{ij}/m$ characterize intra- and interspecies interaction with corresponding two-body scattering lengths $a_{11}\neq a_{22}$ and $a_{12}=a_{21}$.

At this point we introduce dimensionless time and space variables $\tilde{t}=\Omega t$ and $(\tilde{x},\tilde{y},\tilde{z})=(x,y,z)/a_{ho}$ and normalization for the wave functions $\tilde{\psi}_{1,2}=a_{ho}^{3/2}\psi_{1,2}/\sqrt{N_1}$, where $a_{ho}=\sqrt{\hbar/(m\Omega)}$ is the harmonic oscillator strength and $N_{1,2}=\int dV|\psi_{1,2}|^2$ are the numbers of particles. We will consider the quasi-two-dimensional model to simplify our numerical study. This approximation was previously used in several works; see, e.g., [9–11], and is applicable not only for pancake traps, $\sigma\gg 1$, but also captures the main qualitative features of spherical traps. To make a further reduction of Eqs. (1) we redefine the wave functions once more:

$$\tilde{\psi}_{1,2}=\left[\frac{\sigma}{2\pi}\right]^{1/4}\Psi_{1,2}(\tilde{x},\tilde{y},\tilde{t})e^{-\sigma\tilde{z}^2/4}e^{-i\mu_{1,2}\tilde{t}-i\sigma\tilde{t}/2}, \quad (2)$$

where $\mu_{1,2}$ are the chemical potentials. Dropping the tilde we find that equations for $\Psi_{1,2}$ and $\Psi_{1,2}^*$ can be put into Hamiltonian form

$$i\partial_t\vec{\psi}+\hat{\eta}\frac{\delta H}{\delta\vec{\psi}^*}=\vec{0}, \quad (3)$$

$$\vec{\psi}=\begin{bmatrix}\Psi_1\\ \Psi_1^*\\ \Psi_2\\ \Psi_2^*\end{bmatrix}, \quad \hat{\eta}=\begin{bmatrix}-1&0&0&0\\0&1&0&0\\0&0&-1&0\\0&0&0&1\end{bmatrix},$$

$$\frac{\delta H}{\delta\vec{\psi}^*}=\begin{bmatrix}\delta H/\delta\Psi_1^*\\ \delta H/\delta\Psi_1\\ \delta H/\delta\Psi_2^*\\ \delta H/\delta\Psi_2\end{bmatrix},$$

$$H=\int dxdy\Big\{|\vec{\nabla}\Psi_1|^2+|\vec{\nabla}\Psi_2|^2+(\hat{V}-\mu_1)|\Psi_1|^2 + (\hat{V}-\mu_2)|\Psi_2|^2+\frac{g}{2}[\beta_{11}|\Psi_1|^4+\beta_{22}|\Psi_2|^4 + 2\beta_{12}|\Psi_1|^2|\Psi_2|^2]\Big\}. \quad (4)$$

where H is the energy functional (or Hamiltonian), $\vec{\nabla}=\vec{i}_x\partial_x+\vec{i}_y\partial_y$, $\hat{V}=r^2/4$ is the harmonic potential, g is the interaction parameter $g=8\sqrt{\pi\sigma}N_1 a_{11}/a_{ho}$, $\beta_{12}=a_{12}/a_{11}$, and $\beta_{22}=a_{22}/a_{11}$. $\beta_{11}=1$ and it is left in the equations for the sake of symmetry.

Invariancies of H with respect to the infinitesimal rotations and two-parameter phase transformation

$$(\Psi_1,\Psi_2)\rightarrow(\Psi_1 e^{i\phi_1},\Psi_2 e^{i\phi_2}) \quad (5)$$

result in the conservation of the total angular momentum and of the total number of particles in each component.

Radially symmetric stationary states of the condensate (equilibria) can be presented in the form

$$\Psi_j=A_j(r)e^{iL_j\theta}, \quad j=1,2 \quad (6)$$

where θ is the polar angle and A_j are real functions. Using the method suggested in [1,3] only states with a vortex in one of the components can be created, and therefore we will consider below only cases with $L_2>0$ and $L_1=0$. Functions $A_j(r)$ were found numerically using the Newton method. Chemical potentials $\mu_{1,2}$ were found from the normalization conditions

$$2\pi\int rdrA_1^2=1, \quad 2\pi\int rdrA_2^2=\frac{N_2}{N_1}\equiv N. \quad (7)$$

III. FREQUENCY AND ENERGY SPECTRA OF COLLECTIVE EXCITATIONS

A. Bogoliubov equations and the frequency spectrum

To study the spectrum of BECs at equilibrium we linearize Eqs. (3) using substitutions

$$\Psi_j=[A_j(r)+f_j(r,\theta,t)]e^{iL_j\theta}, \quad (8)$$

where f_j are small and complex. Assuming that the excitations are periodic in θ with period 2π, we expand f_j into a Fourier series:

$$f_j=\sum_l [U_{lj}(r,t)e^{il\theta}+V_{lj}^*(r,t)e^{-il\theta}], \quad (9)$$

where $l=0,\pm 1,\pm 2,\ldots$. Then

$$i\partial_t\vec{W}_l+\hat{\eta}\hat{\mathcal{H}}_l\vec{W}_l=\vec{0} \quad (10)$$

is the set of linear partial differential equations resulting from the substitution of Eqs. (8) and (9) into Eq. (3). Here $\vec{W}_l=(U_{l1},V_{l1},U_{l2},V_{l2})^T$,

$$\hat{\mathcal{H}}_l = \begin{bmatrix} \hat{\mathcal{L}}_{l,1} & g\beta_{11}A_1^2 & g\beta_{12}A_1A_2 & g\beta_{12}A_1A_2 \\ g\beta_{11}A_1^2 & \hat{\mathcal{L}}_{-l,1} & g\beta_{12}A_1A_2 & g\beta_{12}A_1A_2 \\ g\beta_{12}A_1A_2 & g\beta_{12}A_1A_2 & \hat{\mathcal{L}}_{l,2} & g\beta_{22}A_2^2 \\ g\beta_{12}A_1A_2 & g\beta_{12}A_1A_2 & g\beta_{22}A_2^2 & \hat{\mathcal{L}}_{-l,2} \end{bmatrix},$$

is a self-adjoint operator and

$$\hat{\mathcal{L}}_{l,j} = -\frac{1}{r}\frac{\partial}{\partial r}r\frac{\partial}{\partial r} + \frac{1}{r^2}(L_j+l)^2 + \hat{V} - \mu_j + 2g\beta_{jj}A_j^2 + g\beta_{12}A_{j'}^2,$$

$$j=1,2, \quad j'=2,1.$$

The frequency spectra of $\hat{\eta}\hat{\mathcal{H}}_l$ are discrete, providing $\hat{V} \neq 0$; therefore, phonons, strictly speaking, are absent in the trap geometry. In accord with standard terminology [4,39], all spatially bounded elementary excitations can be called collective excitations (or collective modes) of an equilibrium under consideration. Linearized equations for excitations in a Bose gas, similar to Eq. (10), were first derived by Bogoliubov, and expansion (9) was first applied in the context of the vortex excitations by Pitaevskii [4]. To find the frequency spectrum and collective modes we need to solve the set of eigenvalue problems

$$\hat{\eta}\hat{\mathcal{H}}_l\vec{w}_{ln} = \omega_{ln}\vec{w}_{ln}. \tag{11}$$

$\hat{\eta}\hat{\mathcal{H}}_l$ are non-self-adjoint operators, and therefore complex frequencies are not forbidden. If $\vec{w}_{ln}$ is an eigenvector of $-\hat{\eta}\hat{\mathcal{H}}_l$ with eigenvalue ω_{ln} it is self-evident that $\vec{w}_{ln}^*$ is also an eigenvector with eigenvalue ω_{ln}^*, and it can be shown that $\hat{\eta}\hat{\mathcal{H}}_{-l}$ has eigenvectors $\vec{w}_{-ln} = \hat{\tau}\vec{w}_{ln}$ and $\vec{w}_{-ln}^*$ with eigenvalues $-\omega_{ln}$ and $-\omega_{ln}^*$, respectively. Here

$$\hat{\tau} = \begin{bmatrix} 0 & 1 & 0 & 0 \\ 1 & 0 & 0 & 0 \\ 0 & 0 & 0 & 1 \\ 0 & 0 & 1 & 0 \end{bmatrix}.$$

Thus the spectrum of $\hat{\eta}\hat{\mathcal{H}}_{-l}$ can be obtained by reflection of the spectrum of $\hat{\eta}\hat{\mathcal{H}}_l$ with respect to the line $\mathrm{Re}\,\omega = 0$ in the plane $(\mathrm{Re}\,\omega, \mathrm{Im}\,\omega)$. In other words, it means that purely real or purely imaginary frequencies of the elementary excitation exist in pairs, complex frequencies exist in quartets, and that

$$\mathrm{Tr}\{\hat{\eta}(\hat{\mathcal{H}}_l + \hat{\mathcal{H}}_{-l})\} = \sum_n (\omega_{ln} + \omega_{-ln}) = 0. \tag{12}$$

Any equilibrium state of the condensate is *spectrally* stable [5] if its spectrum is real. If there is at least one frequency with a negative imaginary part, then the corresponding collective mode will grow in time, destabilizing the equilibrium, which is called spectrally unstable.

B. Biorthogonality

The eigenmodes of $\hat{\eta}\hat{\mathcal{H}}_l$ are biorthogonal to the modes of the adjoint eigenvalue problem [40], i.e.,

$$\langle \vec{w}_{ln}, \vec{a}_{ln'} \rangle = 0, \tag{13}$$

where $n \neq n'$ and $\vec{a}_{ln}$ obey

$$(\hat{\eta}\hat{\mathcal{H}}_l)^\dagger \vec{a}_{ln} = \hat{\mathcal{H}}_l\hat{\eta}\vec{a}_{ln} = \omega_{ln}^*\vec{a}_{ln}, \tag{14}$$

and $\langle \vec{b}, \vec{c} \rangle = 2\pi\Sigma_k\int_0^\infty r dr b_k^* c_k$ for any $\vec{b}$, $\vec{c}$. Factor 2π is introduced to mimic integration over θ. The key feature of our model, originating in its Hamiltonian structure, is that transformation linking $\vec{w}_{ln}$ and its adjoint $\vec{a}_{ln}$ can be found in the explicit and simple form. If $\vec{w}_{ln}$ is an eigenmode of $\hat{\eta}\hat{\mathcal{H}}_l$ with frequency ω_{ln}, then it can be checked that $\hat{\eta}\vec{w}_{ln}^*$ and $\hat{\eta}\vec{w}_{ln}$ are eigenmodes of $\hat{\mathcal{H}}_l\hat{\eta}$ with eigenvalues ω_{ln}^* and ω_{ln}, respectively. The mode adjoint to $\vec{w}_{ln}$ is $\hat{\eta}\vec{w}_{ln}^*$; therefore, if $\mathrm{Im}\,\omega_{ln} \neq 0$, then biorthogonality condition (13) implies

$$\langle \vec{w}_{ln}, \hat{\eta}\vec{w}_{ln} \rangle = 0. \tag{15}$$

If ω_{ln} is real, then $\vec{w}_{ln}$ is also real and $\langle \vec{w}_{ln}, \hat{\eta}\vec{w}_{ln} \rangle \neq 0$. The normalization constant can always be chosen in such a way that

$$|\langle \vec{w}_{ln}, \hat{\eta}\vec{w}_{ln} \rangle| = 2. \tag{16}$$

The convenience of making the left-hand side of Eq. (16) equal to 2 will become clear below, when Eqs. (19),(20) for energies of elementary excitations are derived. Equation (16) makes it explicit that the inner product $\langle \vec{w}_{ln}, \hat{\eta}\vec{w}_{ln} \rangle$ can be either positive or negative. This point often remains silent if one derives conditions similar to Eq. (16) as part of the diagonalization procedure of the second-quantized Hamiltonian, disregarding eigenmodes with negative and zero values of $\langle \vec{w}_{ln}, \hat{\eta}\vec{w}_{ln} \rangle$ [33]. The fact that the inner product of a real eigenmode with its adjoint can be negative is different from standard quantum mechanics based on the self-adjoint operators. These difference can have a series of consequences and one of them is that energy levels are not necessarily linked to the eigenfrequencies according to the standard rule $\hbar\omega$; see below. Note that the origin of the non-self-adjointness in our case is the nonlinearity of GP equations. If particles in the condensate do not interact, $g=0$, then $\hat{\eta}\hat{\mathcal{H}}_l$ become diagonal and self-adjoint.

C. Energy spectrum

As a prelude to the calculation of energies of the elementary excitations it is instructive to introduce the notion of the *nonlinear stability*, i.e., stability under the full nonlinear dynamics. According to Dirichlet's theorem [5], nonlinear stability is ensured if an equilibrium state under consideration is either the minimum or maximum of the functional H. Note here that excitations change the number of particles in the equilibrium state; therefore it was convenient to introduce the energy functional H, which is actually the so-called modified energy [33], i.e., it is the energy functional for Eq. (1) modified by the addition of the number of particles integrals; see terms proportional to μ_j in Eq. (4). To analyze the problem of the nonlinear stability one needs to expand H up to the second order in perturbations, which leads to

$$H = H_0 + \frac{1}{2}\sum_l \langle \vec{w}_l, \hat{\mathcal{H}}_l \vec{w}_l \rangle + \cdots, \tag{17}$$

where H is the energy of the perturbed equilibrium and H_0 is calculated at the exact equilibrium. The equilibrium is nonlinearly stable if the eigenvalue problems

$$\hat{\mathcal{H}}_l \vec{\beta}_{lm} = \alpha_{lm} \vec{\beta}_{lm} \tag{18}$$

have all their eigenvalues either negative or positive, except zero eigenvalues generated by continuous symmetries. Spectral instability implies a nonlinear one, and nonlinear stability implies a spectral one, but not *vice versa* [5]. In the nonrotating traps all the higher-order states of the condensate including vortices are not the local extrema of the energy [19,23,25,27]. Let us stress, however, that their nonlinear instability cannot be guaranteed by this fact alone and requires separate consideration.

If $\vec{w}_l$ in Eq. (17) is an eigenmode $\vec{w}_{ln}$ of $\hat{\eta}\hat{\mathcal{H}}_l$, then

$$\epsilon_{ln} = \frac{1}{2}\langle \vec{w}_{ln}, \hat{\mathcal{H}}_l \vec{w}_{ln} \rangle = \frac{1}{2}\omega_{ln}\langle \vec{w}_{ln}, \hat{\eta}\vec{w}_{ln} \rangle \tag{19}$$

measures energy of this mode. Assuming that ω_{ln} is real and using biorthogonality conditions (16) one gets

$$\epsilon_{ln} = \omega_{ln}\,\mathrm{sgn}\langle \vec{w}_{ln}, \hat{\eta}\vec{w}_{ln} \rangle. \tag{20}$$

If $Im\,\omega_{ln} \neq 0$ then Eq. (15) implies

$$\epsilon_{ln} = 0. \tag{21}$$

The energy in physical units is given by $\epsilon_{ln}\hbar\Omega$.

It is readily demonstrated that

$$\langle \vec{w}_{ln}, \hat{\eta}\vec{w}_{ln} \rangle = -\langle \hat{\tau}\vec{w}_{ln}, \hat{\eta}\hat{\tau}\vec{w}_{ln} \rangle = -\langle \vec{w}_{-ln}, \hat{\eta}\vec{w}_{-ln} \rangle; \tag{22}$$

therefore, modes with frequencies ω_{ln} and $\omega_{-ln} = -\omega_{ln}$ have their energies equal in sign and value.

The eigenfunctions $\vec{\beta}_{ml}$ are orthogonal $\langle \vec{\beta}_{lm}, \vec{\beta}_{lm'} \rangle = \delta_{mm'}$ and form a complete basis. Therefore $\vec{w}_{ln}$ in Eq. (19) can be expanded in terms of $\vec{\beta}_{lm}$, which gives $\epsilon_{ln} = \Sigma_m \alpha_{lm} |\langle \vec{w}_{ln}, \vec{\beta}_{lm} \rangle|^2$. Thus an equilibrium can have collective modes carrying energy with opposite signs only if it is not a local extremum of the energy functional.

D. Resonances and instabilities, crossings and avoided crossings

Instabilities with imaginary eigenvalues have been found to dominate the dynamics of the homogeneous BEC with attractive interaction [6] and the mixture of two condensates with repulsive interaction [7,8]. Higher-order vortices and dark solitons in single-component trapped condensates can be unstable with respect to modes with complex frequencies [9,12]. In our problem, instabilities with complex eigenvalues are the most important ones also. Therefore it is desirable to have a criterion or theorem allowing the interpretation and prediction of these instabilities. Such a theorem is actually known from the general theory of the Hamiltonian dynamical systems [5] and, in our context, it can be reformulated as the following: (i) The sign of the energy of a collective excitation preserves as parameters vary as long as there is no frequency resonance with another excitation. (ii) The condensate at equilibrium can lose spectral stability as parameters vary only in two ways: either via frequency resonance of two elementary excitations with positive and negative energies or by resonance at zero frequency. Proof of these results [5] is based on the fact, that a transition from spectral stability to instability cannot violate the energy conservation law, $\partial_t H = 0$.

From this theorem and preceding considerations one can conclude that the complex eigenvalues in the spectrum of the vortices in the Bose-Einstein condensate can appear only due to mutual annihilation of the collective excitations with positive and negative energies. The theorem does not prohibit the frequencies of two excitations with either the same or opposite signs of the energies from simply crossing each other without change of the spectral stability. In our example it typically happens when corresponding eigenmodes remain orthogonal at the exact resonance. If, however, eigenmodes of the colliding excitations start to compete for the same direction in the functional phase space and become degenerate at the resonance, then crossing is not a generic scenario. If the signs of the energies of the excitations are opposite, then a quartet of complex frequencies appears upon passing the resonance. Alternatively, if the signs are the same, the exact resonance cannot be achieved and it becomes replaced by the so-called avoided crossing of the energy levels [5].

Figures 1(a) and 1(b) show numerically calculated frequency and energy spectra of the collective excitations with $l = \pm 1$ for spectrally stable (left panel) and spectrally unstable (right panel) unit vortices ($L_1 = 0$, $L_1 = 1$). The negative-energy excitation is clearly seen in the spectrally stable situation. At the transition threshold to spectral instability this excitation and another one, having energy with the same absolute value but opposite sign, annihilate each other. This transition is accompanied by the appearance of the zero energy excitations. Examples of frequency and energy evolution under the parameter variation resulting in instabilities, crossings, and avoided crossing are given in Sec. IV. Figures 1(c) show the spectra of $\hat{\mathcal{H}}_{\pm 1}$. There are no qualitative changes in these spectra after the appearance of complex frequencies.

The possibility of the observation of collective modes with complex frequencies has caused some concerns and discussions [12,27]. However, initial perturbations of the equilibrium state having nonzero projections on the adjoint mode $\hat{\eta}\vec{w}^*_{ln}$ with $\mathrm{Im}\,\omega^*_{ln} > 0$ will lead to the ultimate growth of the corresponding mode $\vec{w}_{ln}$ because it has $\mathrm{Im}\,\omega_{ln} < 0$. The consequences of this growth is in no way diminished by the fact

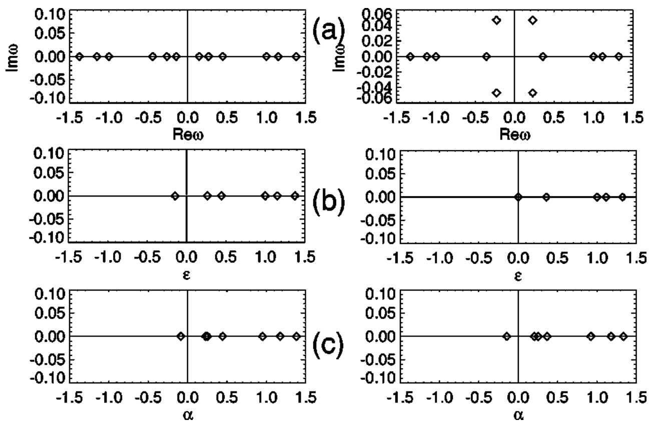

FIG. 1. Numerically calculated frequency (a) and energy (b) spectra corresponding to the collective modes with $l=\pm 1$ of the spectrally stable (left panel) and spectrally unstable (right panel) unit vortices: $L_1=0$, $L_2=1$, $g=250$, $N=1$; other parameters for the left/right panel correspond to the vortex in the state 1/state 2, see text after Eq. (32). The correspondence between frequency and energy spectra is obvious; see Eqs. (20), (21). (c) Spectrum of the eigenvalue problems $\hat{\mathcal{H}}_{\pm 1}\vec{\beta}_n=\alpha_n\vec{\beta}_n$; parameters, as for (a),(b).

that the energy of this mode is zero. A wealth of references and examples of instabilities with complex eigenvalues existing in other physical contexts can be found in [5,43].

E. Goldstone and dipole modes

Infinitesimal variations of ϕ_j, see Eq. (5), generate two zero-energy eigenmodes (Goldstone modes) $(A_1, -A_1,0,0)^T$ and $(0,0,A_2,-A_2)^T$ belonging to the null eigenspace of $\hat{\eta}\hat{\mathcal{H}}_0$. Harmonic trapping modifies the spectrum in such a way that $\hat{\eta}\hat{\mathcal{H}}_{\pm 1}$ acquire a couple of parameter-independent eigenvalues $\omega=\pm 1$ with eigenfunctions

$$\vec{w}_{\pm 1d}=\begin{bmatrix} \omega\left(\dfrac{dA_1}{dr}\mp\dfrac{1}{r}L_1A_1\right)+\dfrac{1}{2}rA_1 \\ \omega\left(\dfrac{dA_1}{dr}\pm\dfrac{1}{r}L_1A_1\right)-\dfrac{1}{2}rA_1 \\ \omega\left(\dfrac{dA_2}{dr}\mp\dfrac{1}{r}L_2A_2\right)+\dfrac{1}{2}rA_2 \\ \omega\left(\dfrac{dA_2}{dr}\pm\dfrac{1}{r}L_2A_2\right)-\dfrac{1}{2}rA_2 \end{bmatrix}, \tag{23}$$

where ω can take values of ± 1 for both eigenmodes. $\vec{w}_{\pm 1d}$ are often called dipole modes and $\epsilon_{\pm 1d}=1$. Equations (23) generalize expressions previously derived for single-species condensates [23]. The existence of the dipole modes can also be associated with Kohn's theorem [41,42].

IV. COLLECTIVE EXCITATIONS OF UNIT VORTICES: $L_1=0$, $L_1=1$

We begin our analysis considering a weakly interacting condensate: $g\ll 1$, $N\sim 1$. In this limit potential energy due to harmonic trapping $\hat{V}$ strongly dominates over the interaction energy, which allows one to make explicit calculations of the frequency and energy spectra of the elementary excitations. Calculations of the excitation spectra of the vortices and dark solitons in the single-component weakly interacting condensates have been recently done by several groups of authors [12,25]. However, these calculations lack an analysis of the energy sign in the sense explained in the preceding section.

We substitute asymptotic expansions $\mu_{1,2}=\mu_{1,2}^{(0)}+g\mu_{1,2}^{(1)}+O(g^2)$, $A_{1,2}=A_{1,2}^{(0)}+gA_{1,2}^{(1)}+O(g^2)$ into the stationary $(\partial_t=0)$ version of Eqs. (3) and derive a recurrent system of linear equations. In the zero approximation we have two uncoupled harmonic-oscillator problems with eigenmodes

$$A_1^{(0)}=\frac{1}{\sqrt{2\pi}}e^{-r^2/4},\quad A_2^{(0)}=\sqrt{\frac{N}{\pi}}\frac{r}{2}e^{-r^2/4}. \tag{24}$$

Using the solvability condition of the first-order problem we find asymptotic expressions for the chemical potentials: $\mu_1=1+g(2\beta_{11}+n\beta_{12})/(8\pi)+O(g^2)$, $\mu_2=2+g(n\beta_{22}+\beta_{12})/(8\pi)+O(g^2)$.

Then we expand the operators $\hat{\mathcal{H}}_l$, eigenmodes $\vec{w}_l$, and frequencies ω_l into the series $\hat{\mathcal{H}}_l=\hat{\mathcal{H}}_l^{(0)}+g\hat{\mathcal{H}}_l^{(1)}+O(g^2)$, $\vec{w}_l=\vec{w}_l^{(0)}+g\vec{w}_l^{(1)}+O(g^2)$, $\omega_l=\omega_l^{(0)}+g\omega_l^{(1)}+O(g^2)$. After substitution into Eq. (11) in the first order, we find the standard equation

$$(\hat{\eta}\hat{\mathcal{H}}_l^{(0)}-\omega_l^{(0)})\vec{w}_l^{(1)}=(\omega_l^{(1)}-\hat{\eta}\hat{\mathcal{H}}_l^{(1)})\vec{w}_l^{(0)}. \tag{25}$$

$\hat{\eta}\hat{\mathcal{H}}_l^{(0)}$ is diagonal and self-adjoint and all its eigenmodes and eigenvalues can be found explicitly. Then using the solvability condition for Eq. (25) one can find corrections for all frequencies and coefficients in the linear superposition of the zero approximation eigenmodes. Computer algebra makes the technical realization of this plan a straightforward exercise. We will present and analyze explicit analytical results only for the operator $\hat{\eta}\hat{\mathcal{H}}_{-1}$ considering the vicinity of the spectral point $\omega=1$, because it contains information about the origin of the spectral instabilities of unit vortices. An equivalent analysis of $\hat{\eta}\hat{\mathcal{H}}_1$ near $\omega=-1$ gives the same results.

$\hat{\eta}\hat{\mathcal{H}}_{-1}^{(0)}$ has three unit frequencies, $\omega_{-1}^{(0)}=1$. The corresponding eigenmodes are

$$\vec{b}_1=(0,1,0,0)^T\frac{r}{2\sqrt{\pi}}e^{-r^2/4},$$
$$\vec{b}_2=(0,0,1,0)^T\frac{1}{\sqrt{2\pi}}e^{-r^2/4}, \tag{26}$$
$$\vec{b}_3=(0,0,0,1)^T\frac{r^2}{4\sqrt{\pi}}e^{-r^2/4}.$$

The solvability conditions for Eq. (25) lead to the characteristic determinant of the three by three matrix. We find that one of the three frequencies is associated with the dipole mode $\vec{w}_{-1d}$ and that the other two are

$$\omega_{-1}^{\pm}=1+\frac{g}{32\pi}(-3\beta_{12}-N\beta_{22}\pm\sqrt{R})+O(g^2), \quad (27)$$

$$R\equiv(3\beta_{12}+N\beta_{22})^2-8\beta_{12}^2(N+1).$$

The corresponding unnormalized eigenmodes are

$$\vec{w}_{-1}^{\pm}=\sqrt{2N}(N\beta_{22}-\beta_{12}\pm\sqrt{R})\vec{b}_1 + \sqrt{2}(3N\beta_{22}+[1-4N]\beta_{12}\mp\sqrt{R})\vec{b}_2 + 4N(\beta_{12}-\beta_{22})\vec{b}_3+O(g). \quad (28)$$

The pair of frequencies (27) becomes complex if $R<0$, signaling a spectral instability of the unit vortex. If $R>0$, then

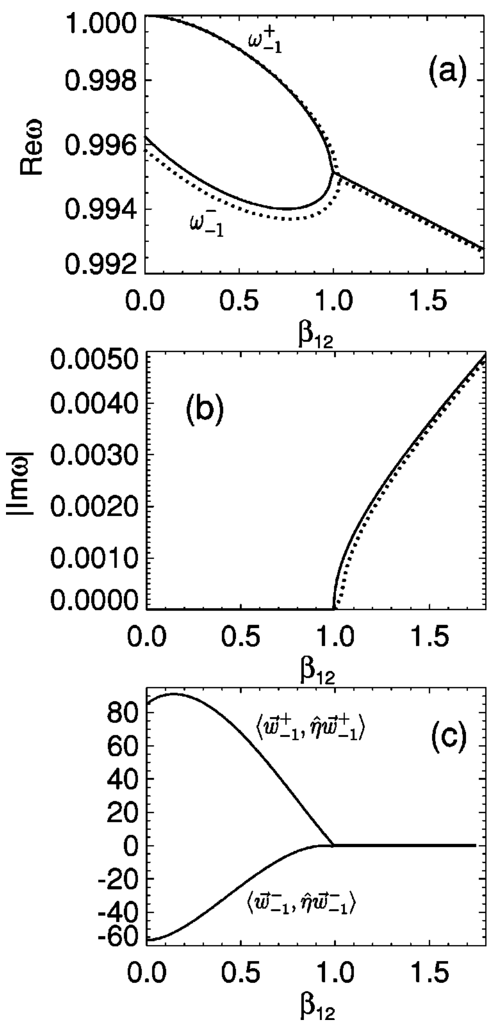

FIG. 2. (a),(b) Frequencies $\omega_{-1}^{\pm}$ vs β_{12}: $N=2$, $g=0.1$, $\beta_{22}=0.97/1.03$. (c) Inner products $\langle\vec{w}_{-1}^{\pm},\hat{\eta}\vec{w}_{-1}^{\pm}\rangle$ characterizing energy signs of the corresponding excitations; see Eq. (30). The dotted lines are numerical solutions of $\hat{\eta}\hat{\mathcal{H}}_{-1}\vec{w}_l=\omega_l\vec{w}_l$ and the full lines correspond to Eqs. (28) and (30).

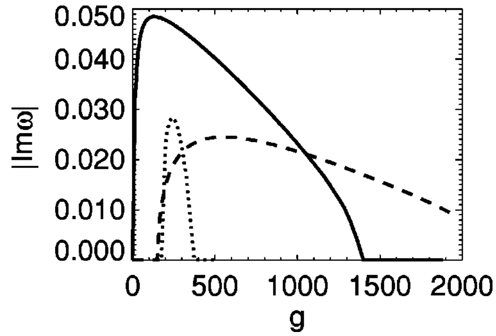

FIG. 3. Instability growth rate of the unit vortex in state 2 vs the interaction parameter g. The full line, $N=1$; the dashed line, $N=0.3$; the dotted line, $N=9$.

$$\langle\vec{w}_{-1}^{\pm},\hat{\eta}\vec{w}_{-1}^{\pm}\rangle= 4[R(N-1)\pm\sqrt{R}\{(1-5N)\beta_{12}+N(3+N)\beta_{22}\}] \quad (29)$$

and one can check that

$$\epsilon_{-1}^{\pm}=\pm\omega_{-1}^{\pm}, \quad (30)$$

i.e., modes with frequencies ω_{-1}^{+} and ω_{-1}^{-} have, respectively, positive and negative energies; see Fig. 2(c). One can also verify biorthogonality $\langle\vec{w}_{-1}^{\pm},\hat{\eta}\vec{w}_{-1}^{\pm}\rangle=0=\epsilon_{-1}^{\pm}$ for $R<0$, see Eq. (15), and $\langle\vec{w}_{-1}^{\pm},\hat{\eta}\vec{w}_{-1}^{\mp}\rangle=0$ for $R>0$, see Eq. (16).

Assuming $\beta_{ij}>0$ and rewriting the instability condition $R<0$ in the form

$$\frac{\beta_{22}}{\beta_{12}}<\frac{1}{N}(2\sqrt{2(N+1)}-3), \quad (31)$$

one can see that unit vortices are more stable if the intraspecies interaction of atoms in the vortex containing part of the condensate is somewhat larger than the interspecies interaction. The choices of scattering lengths corresponding to the experiment [1] are $\beta_{22}=1.03/0.97$, $\beta_{12}=1/0.97$ $(\beta_{22}>\beta_{11})$ and $\beta_{22}=0.97/1.03$, $\beta_{12}=1/1.03$ $(\beta_{22}<\beta_{11})$. The former case corresponds to the vortex in the spin state $\{F=1,m_f=-1\}$ of ^{87}Rb and the latter to the vortex in the state $\{2,2\}$. These two states will be called state 1 and state 2. It is clear that for $N=1$ Eq. (31) predicts instability for the vortex in state 2 and stability for the vortex in state 1, which supports the results of the experimental observations [1].

Figure 2 shows frequency resonance accompanied by the simultaneous mutual annihilation of excitations with positive and negative energies happening at some critical value of β_{12}; see Eq. (31). In fact, it models the transition from the situation with vortex in state 1 to the case with vortex in state 2. Performing numerical studies for a wide range of parameters, outside the validity region of analytical considerations, we have not been able to find regions of spectral instability of the unit vortex in state 1. Contrarily, the existence of instabilities of the vortex in state 2 due to exactly the same scenario, which is predicted in the weak interaction limit, can be readily demonstrated; see Fig. 3.

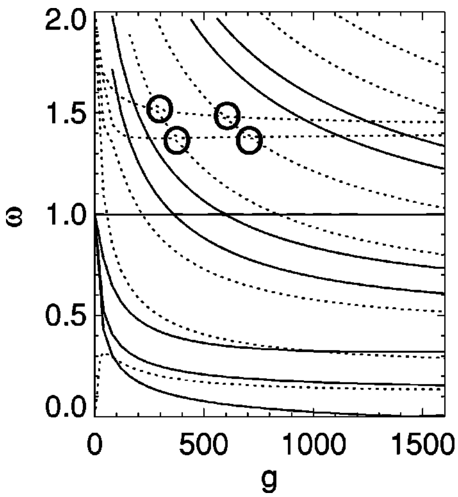

FIG. 4. Positive part of the frequency spectrum of the collective excitations with $|l|=1$ (full lines) and $|l|=2$ (dotted lines) of the unit vortex in state 1 vs the interaction parameter g: $N=1$. Open circles mark the avoided crossings (i.e., avoided frequency resonances) of the excitation with positive energies.

It is important to stress that, if two condensates are decoupled, $\beta_{12}=0$, then the negative-energy mode $\vec{w}_{-1}^{-}$ belongs to the vortex-containing component and the positive-energy mode $\vec{w}_{-1}^{+}$ belongs to the vortex-free component. Because of this separation, the instability is not possible for any values of g, which agrees with spectral stability of unit vortices in the single-component case reported in [9]. Thus we can conclude that the vortex instability in our example has essentially a two-component nature and its analog may also exist in the case when the second component is a noncondensate one.

A criterion similar to Eq. (31), but without a corresponding energy analysis, has also been independently obtained in [11] using the two-mode approach, i.e., condensate wave functions Ψ_1 and Ψ_2 have been presented as the linear superposition of modes (24) with time-dependent coefficients and GP equations having been reduced to the set of ordinary differential equations for these coefficients [11]. However, this method fails to take into account an eigenmode proportional to r^2, see $\vec{b}_3$ in (26), which makes an important contribution to the expressions for frequencies. Therefore, Eqs. (27) and (31) are different from the corresponding results presented in [11].

To illustrate the crossings and avoided crossings in the spectrum of unit vortices we show in Fig. 4 the positive part of the frequency spectra of $\hat{\eta}\hat{\mathcal{H}}_{\pm 1}$ and $\hat{\eta}\hat{\mathcal{H}}_{\pm 2}$. One can see numerous points, which at first glance can be interpreted as crossings in the frequency spectrum. However, under close investigation, those that are marked by open circles, turn out to be the avoided crossing of the excitations with equal energy signs; see Fig. 5.

V. DRIFT OF UNIT VORTICES

The unstable modes of the vortex in state 2 are of the dipole type, i.e., $|l|=1$; therefore their growth leads to the initial displacement of the vortex from the trap center. The displaced vortex carries less of the total angular momentum, compared to the momentum of the vortex positioned at the trap center. A lack of angular momentum is compensated by two factors. First, the vortex acquires a nonzero tangential velocity and therefore its trajectory is actually a spiral, which is similar to the dynamics of an optical vortex displaced from the center of a Gaussian beam [44]. Second, angular momentum, and the vortex itself, become gradually transferred into the second condensate component, which was first demonstrated in [10,11].

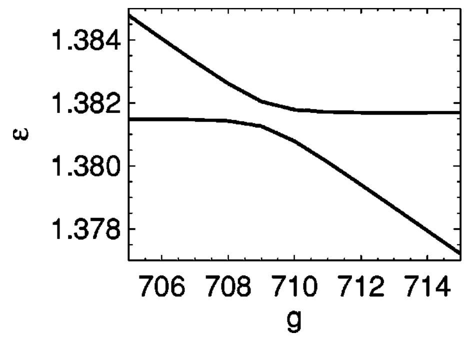

FIG. 5. Dependencies of energies of two elementary excitations with $l=2$ vs g showing details of the rightmost from the avoided crossings marked in Fig. 4.

If drift instability is absent, then dissipative effects still can result in the vortex drift, which was predicted for the single-component condensates by several authors [19,32]. The presence of the second condensate opens a channel for the energy and angular-momentum transfer from the vortex into the vortex-free component. It can be seen that the vector $\vec{b}_1$, being excited by the instability, provides a channel for this transfer. Thus drift instability can also be interpreted as due to dissipation of the energy and momentum by the vortex-free condensate component.

In the limits $N\gg 1$ and $N\ll 1$ our model can be approximately considered as a single-component condensate with ($N\gg 1$) or without ($N\ll 1$) a vortex. The unit vortex and ground state of the single-component condensate are known to be spectrally stable. Therefore drift instability disappears in both limits; see Fig. 3. An increase of g for fixed N also results in the suppression of the instability, see Fig. 3, which

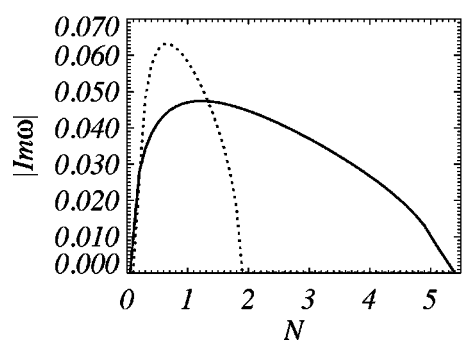

FIG. 6. Growth rate of the drift $|l|=1$ (full lines) and splitting $|l|=2$ (dotted lines) instabilities of the double vortex in state 2 vs N for $g=900$.

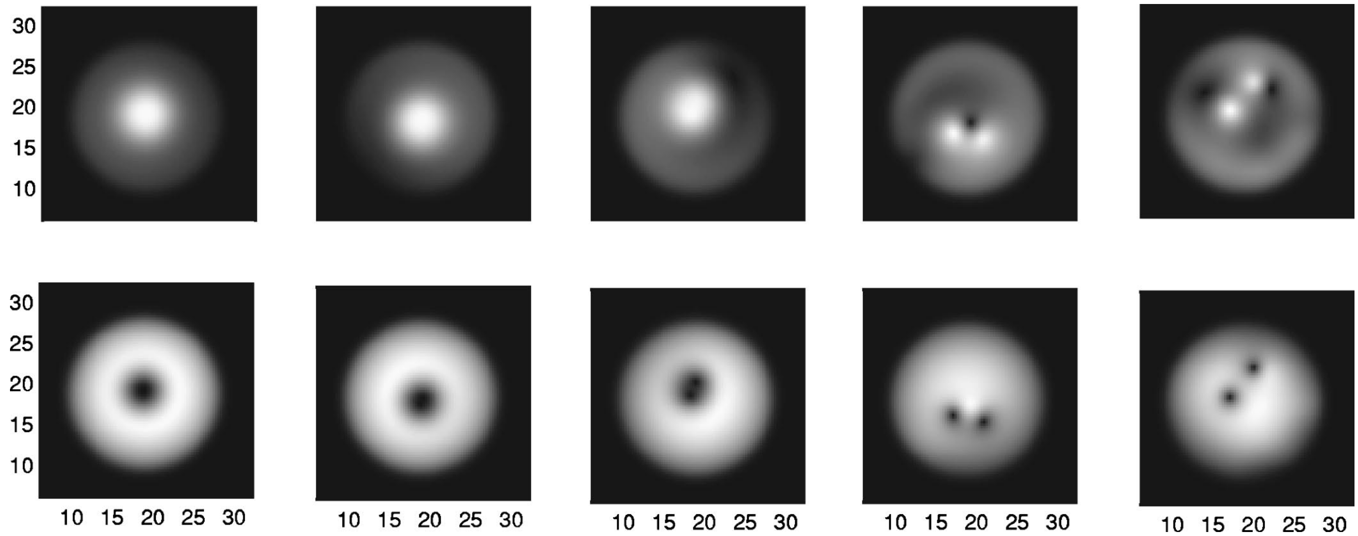

FIG. 7. Development of the drift instability of the double vortex in state 2: $g=900$, $N=2.5$. Top, $|\Psi_1(x,y)|^2$; bottom, $|\Psi_2(x,y)|^2$. The time interval between snapshots is 20. The first snapshot corresponds to $t=60$.

means that not only a relative, but also an absolute, increase of the number of atoms in the vortex-free component stabilizes the condensate.

VI. DRIFT AND SPLITTING OF HIGHER-ORDER VORTICES

Considering higher-order vortices one can expect to find an instability scenario resulting in their splitting into unit vortices. This scenario is expected to be due to a growth of the collective modes with $|l|>1$. However, as we will see below the drift instability linked to the dipolelike modes, $|l|=1$, can also be presented. It leads to displacement of the whole vortex from the trap center without splitting, at least at the onset of the instability.

Both the drift and splitting instabilities of the higher-order vortices appear as a result of the frequency resonances of the elementary excitations with negative and positive energies, similar to the case of unit vortices. $N\ll 1$ corresponds to the vortex-free condensate, and therefore both instabilities disappear in this limit. In the limit $N\gg 1$ only drift instability is suppressed and one can recover periodic in N bands of the instabilities with complex frequencies and $|l|>1$, similar to the results reported for higher-order vortices in a single-component condensate [9]. Note, that splitting itself was not explicitly demonstrated in [9]. It is also interesting to note that higher-order vortices in the free, $\hat{V}=0$, single-component condensate are spectrally stable [45]. Thus splitting can be considered as induced by the trapping. The vortex-free condensate component plays a crucial role in the drift instability, but whether the latter one will be presented without trapping or not remains an open problem.

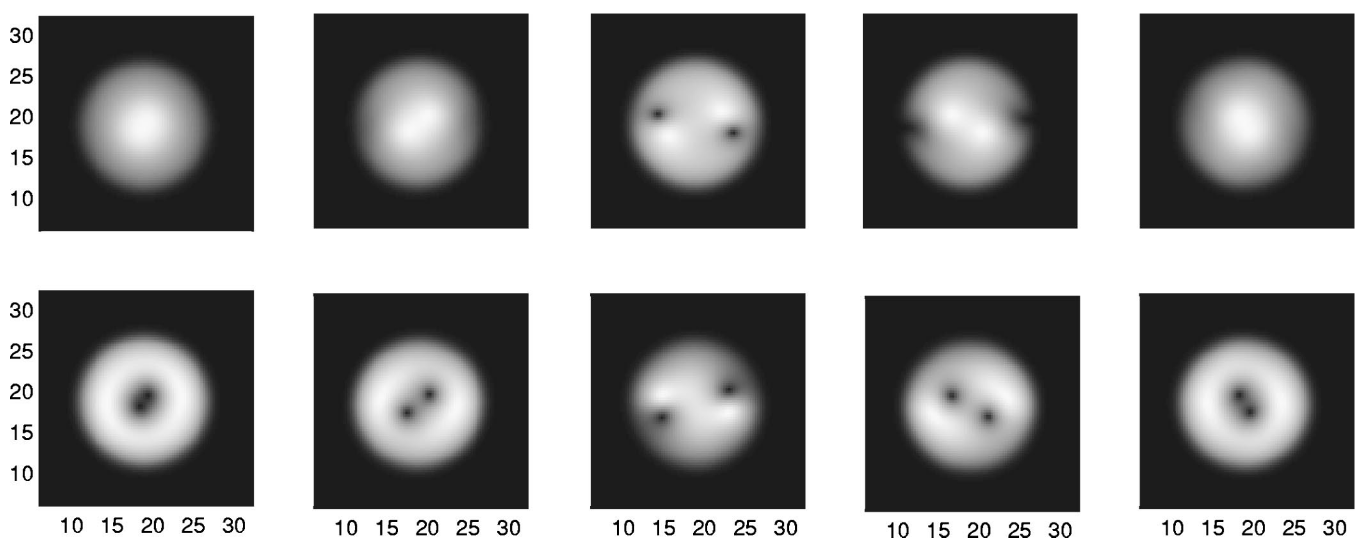

FIG. 8. Development of the splitting instability of the double vortex in state 2: $g=900$, $N=0.7$. Top, $|\Psi_1(x,y)|^2$; bottom, $|\Psi_2(x,y)|^2$. The time interval between snapshots is 20. The first snapshot corresponds to $t=30$.

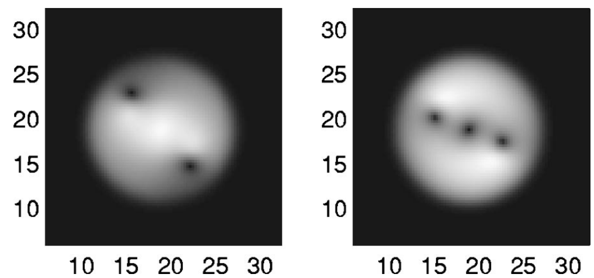

FIG. 9. $|l|=2$ instability of the triple vortex in state 2: $g=900$, $N=0.9$, $t=70$. Left, $|\Psi_1(x,y)|^2$; right, $|\Psi_2(x,y)|^2$.

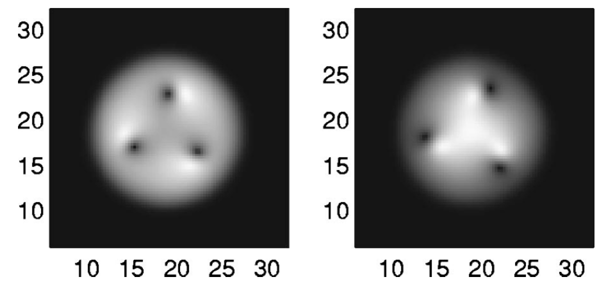

FIG. 10. $|l|=3$ instability of the triple vortex in state 2: $g=900$, $N=0.9$, $t=85$. Left, $|\Psi_1(x,y)|^2$; right, $|\Psi_2(x,y)|^2$.

A. Double vortices: $L_1=0$, $L_2=2$

Considering the double vortex, we have found that it can be unstable with respect to the $|l|=1,2$ excitations. The vortex in state 1 has been found to be surprisingly stable. One has to take relatively small values of g and large N to find splitting instability. The vortex in state 2 is more unstable in the sense that splitting exists already for $N\sim 1$; see Fig. 6. As is evident from Fig. 6, either drift or splitting instability can dominate vortex dynamics. If drift instability is dominant, then the vortex first gets displaced from the trap center and only then splits into the unit ones; see Fig. 7. The latter happens due to the curved background that breaks cylindrical symmetry with respect to the vortex axis. Afterwards, the splitting vortices remain close to each other and move towards the condensate periphery. Results of the numerical simulation of the GP equations (1) presented in this section were obtained starting from equilibrium states perturbed by random noise with amplitude $\sim 0.05A_{1,2}$.

The dynamics is quite different when the splitting instability is dominant; see Fig. 8. In this case unit vortices appear straight at the onset of the instability development and spiral out of the condensate center, always being positioned symmetrically with respect to it. After a certain period of time vortices move back to the trap center and the condensate state close to the initial one is restored, see Fig. 8; then the cycle is repeated with a gradually worsening degree of periodicity.

During the development of the instability, angular momentum becomes partially transferred into the second condensate. An analysis of the transverse profiles of the phases corresponding to the density profiles shown in Fig. 8 has revealed that black spots appearing in the second condensate are indeed unit vortices, not the density holes without topological structure.

B. Triple vortices: $L_1=0$, $L_2=3$

A rich variety of beautiful vortex lattices can be found considering instabilities of vortices of the order 3 and higher. This richness can be understood in terms of spatial profiles of the unstable collective modes. E.g., the triple vortex has been found to be unstable with respect to the perturbations with $|l|=1,2,3$. All components of the $|l|=2$ excitations are equal to zero at the trap center. Therefore one can expect that the growth of this mode will develop into a spatial structure preserving the vortex at the trap center. Contrarily some of the components of the $|l|=3$ modes have humps at the center. Therefore their growth should repel all unit vortices out of the center, which leads to the breaking of the triple vortex into a triangular structure of the unit vortices moving away from the trap center. Both instabilities can be found for the same parameters values and can have close growth rates. Therefore the winning mode is selected through the process of complex competition; see Figs. 9 and 10.

VII. SUMMARY

We have described the general approach to the stability of equilibrium in a BEC using Bogoliubov theory and GP equation. Biorthogonality conditions (15) and (16) and the correspondence between frequency and energy spectra of the elementary excitations (20) and (21) have been derived selfconsistently from first principals revealing several alternative and conceptually important aspects.

It has been demonstrated that frequency resonances of the excitations with positive and negative energies can lead to their mutual annihilation and the appearance of collective modes with complex frequencies and zero energies. Conditions for the avoided crossing of energy levels have also been discussed. The general theory has been verified both numerically and analytically in the weak interaction limit, considering an example of vortices in a binary mixture of condensates.

The growth of excitations with complex frequencies leads to the two main scenarios of the instability development. The first one is the spiraling of the unit and double vortices out of the condensate center to its periphery. The second scenario is the splitting of the double- and higher-order vortices into unit ones. An absolute and/or relative increase of the number of particles in the vortex-free condensate component has been found to have a stabilizing effect.

ACKNOWLEDGMENTS

The author acknowledges discussions with S. M. Barnett and W. J. Firth. The numerical part of the work was significantly speeded up due to access to the computer equipment obtained via U.K. EPSRC Grant No. GR/M31880 and the assistance of G. Harkness and R. Martin.

[1] M. R. Matthews, B. P. Anderson, P. C. Haljan, D. S. Hall, C. E. Wieman, and E. A. Cornell, Phys. Rev. Lett. **83**, 2498 (1999).
[2] K. W. Madison, F. Chevy, W. Wohlleben, and J. Dalibard, Phys. Rev. Lett. **84**, 806 (2000).
[3] J. E. Williams and M. J. Holland, Nature (London) **401**, 568 (1999).
[4] L. P. Pitaevskii, Zh. Exp. Teor. Fiz. **40**, 646 (1961) [Sov. Phys. JETP **13**, 451 (1961)].
[5] R. S. MacKay, in *Hamiltonian Dynamical Systems*, edited by R. S. MacKay and J. D. Meiss (Hilger, Bristol, 1987), p. 137.
[6] N. Bogolubov, J. Phys. (USSR) **11**, 23 (1947).
[7] E. A. Goldstein and P. Meystre, Phys. Rev. A **55**, 2935 (1997).
[8] E. Timmermans, Phys. Rev. Lett. **81**, 5718 (1998).
[9] H. Pu, C. K. Law, J. H. Eberly, and N. P. Bigelow, Phys. Rev. A **59**, 1533 (1999).
[10] J. J. Garcia-Ripoll and V. M. Pérez-Garcia, Phys. Rev. Lett. **84**, 4264 (2000).
[11] J. J. Garcia-Ripoll and V. M. Pérez-Garcia, Phys. Rev. A **62**, 033601 (2000).
[12] D. L. Feder, M. S. Pindoza, L. A. Collins, B. I. Schneider, and C. W. Clark, e-print cond-mat/0004449.
[13] In the mathematical literature the energy sing is often called *signature* of the eigenvalue.
[14] K. Weierstrass, *in Weierstrass: Mathematische Werke*, Vol. 1 (Johnson, New York, 1967), p. 233.
[15] A. Hasegawa, *Plasma Instabilities and Nonlinear Effects* (Springer, Berlin, 1975), p. 18.
[16] R. S. MacKay and P. G. Saffman, Proc. R. Soc. London, Ser. A **406**, 115 (1986).
[17] M. Edwards, R. J. Dodd, C. W. Clark, P. A. Ruprecht, and K. Burnett, Phys. Rev. A **53**, R1950 (1996).
[18] F. Dalfovo and S. Stringari, Phys. Rev. A **53**, 2477 (1996).
[19] D. S. Rokhsar, Phys. Rev. Lett. **79**, 2164 (1997).
[20] S. Sinha, Phys. Rev. A **55**, 4325 (1997).
[21] R. J. Dodd, K. Burnett, M. Edwards, and C. W. Clark, Phys. Rev. A **56**, 587 (1997).
[22] F. Zambelli and S. Stringari, Phys. Rev. Lett. **81**, 1754 (1998).
[23] A. A. Svidzinsky and A. L. Fetter, Phys. Rev. A **58**, 3168 (1998); A. A. Svidzinsky and A. L. Fetter, Phys. Rev. Lett. **84**, 5919 (2000).
[24] E. Lundh, C. J. Pethick, and H. Smith, Phys. Rev. A **58**, 4816 (1998).
[25] M. Linn and A. L. Fetter, Phys. Rev. A **60**, 4910 (1999).
[26] D. L. Feder, C. W. Clark, and B. Schneider, Phys. Rev. Lett. **82**, 4956 (1999).
[27] J. J. Garcia-Ripoll and V. M. Pérez-Garcia, Phys. Rev. A **60**, 4864 (1999).
[28] D. L. Feder, C. W. Clark, and B. Schneider, Phys. Rev. A **61**, 011 601 (2000).
[29] B. Jackson, J. F. McCann, and C. S. Adams, Phys. Rev. A **61**, 013 604 (2000).
[30] T. Isoshima and K. Machida, Phys. Rev. A **59**, 2203 (1999).
[31] S. Stringari, Phys. Rev. Lett. **82**, 4371 (1999).
[32] P. O. Fedichev and G. V. Shlyapnikov, Phys. Rev. A **60**, R1779 (1999).
[33] A. L. Fetter, Ann. Phys. (N.Y.) **70**, 67 (1972).
[34] W. B. Colson and A. L. Fetter, J. Low Temp. Phys. **33**, 231 (1978).
[35] T.-L. Ho and V. B. Shenoy, Phys. Rev. Lett. **77**, 3276 (1996).
[36] C. K. Law, H. Pu, N. P. Bigelow, and J. H. Eberly, Phys. Rev. Lett. **79**, 3105 (1997).
[37] B. D. Esry and C. H. Greene, Phys. Rev. A **59**, 1457 (1999).
[38] P. Öhberg, Phys. Rev. A **59**, 634 (1999).
[39] P. Noziéres and D. Pines, *The Theory of Quantum Liquids. Vol. II. Superfluid Bose Liquid* (Perseus Books, Cambridge, 1999), p. 169.
[40] P. M. Morse and H. Feshbach, *Methods of Theoretical Physics, Part 1* (McGraw-Hill, New York, 1953), p. 884.
[41] W. Kohn, Phys. Rev. **123**, 1242 (1961).
[42] J. F. Dobson, Phys. Rev. Lett. **73**, 2244 (1994).
[43] D. V. Skryabin, Physica D **139**, 186 (2000); D. V. Skryabin, Phys. Rev. E **60**, 7511 (1999); D. V. Skryabin and W. J. Firth, *ibid.* **58**, R1252 (1998); **58**, 3916 (1998).
[44] Y. S. Kivshar, J. Christou, V. Tikhonenko, B. Luther-Davies, and L. M. Pismen, Opt. Commun. **152**, 198 (1998).
[45] I. Aranson and V. Steinberg, Phys. Rev. B **53**, 75 (1996).